buildings

Article

Porosity-to-Cement Index Controlling the Strength and Microstructure of Sustainable Crushed Material-Cemented Soil Blends

Jair A. Baldovino [1,*], Carlos Millan-Paramo [2] and Manuel Saba [3]

1 Grupo de Investigación en Geotecnia Aplicada, Civil Engineering Program, Faculty of Engineering, Universidad de Cartagena, Cartagena de Indias 130015, Colombia
2 ESTROPTI Research Group, Department of Civil Engineering, Universidad de Sucre, Sincelejo 700003, Colombia
3 Grupo de Investigación ESCONPAT, Civil Engineering Program, Faculty of Engineering, Universidad de Cartagena, Cartagena de Indias 130015, Colombia
* Correspondence: jarrietab2@unicartagena.edu.co; Tel.: +57-3042602846

Abstract: Recently, studies that introduce alternative binders or wastes for created geo-materials that can be mixed with soil to give it greater strength, are of paramount importance. Roof tile residue, for example, has been widely used to create geopolymers in mortar and concrete. However, its application to soil stabilization has been limited. Additionally, there are no recent studies on the design of soil-tile mixtures with criteria, based on the estimation indexes of mechanical resistance, durability, and microstructure. Thus, this paper introduces another new geo-material not studied in the current literature: crushed roof tile (RT) waste mixed with soil-cement. For this, sedimentary soil was mixed with cement (C) and RT in various quantities and cured under 28 days. The influence and impact of the porosity/cement index (η/C_{iv}) on the split tensile (q_t) and compressive (q_u) strengths were studied. Concerning porosity, as well as the cement content, it had a strong influence on strength. Regardless of the cement content used, a decrease in the material's porosity promoted considerable gains in strength due to a more significant number of contacts between particles and a more outstanding interlocking between the soil particles. In addition, the greater ability to distribute stresses within the geomaterial compacted specimen and the greater capacity to mobilize friction in lower porosity states to contribute to the strength of the RT-soil-cement mixture. The index split tensile/compression was calculated as 0.18, independent of cement and the RT content. During the chemical microanalysis, the soil particles and the RT detected the cementing material between the soil particles. Finally, the new geomaterial can be applied to several uses in geotechnical engineering. From an environmental point of view, the RT-soil blends are considered technically sustainable. Reconciling sustainability and the development of new materials is, without a doubt, essential for us to progress in society. Cemented soil with RT residues have emerged recently and are a potential replacement for traditional materials, as demonstrated in this paper.

Keywords: porosity/cement index; roof tile waste; sustainable; reuse; geo-materials

check for updates

Citation: Baldovino, J.A.; Millan-Paramo, C.; Saba, M. Porosity-to-Cement Index Controlling the Strength and Microstructure of Sustainable Crushed Material-Cemented Soil Blends. *Buildings* **2022**, *12*, 1966. https://doi.org/10.3390/buildings12111966

Academic Editor: Jian-Guo Dai

Received: 15 October 2022
Accepted: 9 November 2022
Published: 12 November 2022

1. Introduction

In recent decades, cement replacement from waste use has shown to be an alternative with a great potential for soil improvement, since it provides excellent mechanical yields. To obtain this new cementing material, the inclusion of various industrial and domestic waste and by-products, as the primary source of raw material, should be highlighted, which contributes to a sustainable development where the exploitation of natural resources is stopped, and the problems of the final disposal of waste are bypassed [1–3].

The term soil stabilization is understood as an artificial method used to improve by the appropriate reclassification or by the notable additions of such properties of soil, that are of extreme interest for the conservation of shear strength, volume, and shape of the soil ground [4]. Among the properties that can be changed, we can mention resistance, rigidity, compressibility, permeability, workability, sensitivity to water, tendency to change volume, swelling potential, and susceptibility to ice. In its broadest meaning, soil stabilization encompasses all physical, physicochemical, and chemical methods used to make the soil to better serve its intended engineering purpose [5]. In its more specific definition, for example, for road engineering, soil stabilization is the name given to construction techniques in which soils are treated to provide their use in sub-bases, bases, and, in some rare cases, surface courses, which can withstand loads of traffic and wet conditions throughout their lifetime [6]. The alteration of the natural properties of the soil in such a way that it creates a material competent to respond to the established design requests defines the technique of soil stabilization. It is based on the treatment of the soil, whether by a mechanical, physical, or chemical processes, making it stable for the limits of its use, and keeping it that way, even under the action of external loads (for example, the rotation of traffic) and weather conditions [7].

Using ceramic waste from both civil construction waste and the production process (damaged parts), becomes an attractive option because, in addition to solving problems related to the disposal in sanitary landfills, they can help in the partial or total replacement of Portland cement [8]. Despite these studies proving ceramic residues as a precursor material for alkali activation, they have in common the need for high curing temperatures for the activation process to occur and to obtain significant compressive strength values [9]. For this reason, Robayo et al. [10] studied the use of the NaOH activator solution in different Na_2O contents, concerning the mass of ceramic residue. To achieve the best compressive strength, this optimum content was 10%, providing a value of 7.49 MPa and 15.57 MPa, cured at 25 °C and 70 °C, respectively, for 48 h first, and after 28 days of dry curing. The incorporation of soluble silica into the alkaline activator showed a positive effect, reaching 54.38 MPa of compressive strength when cured at 25 °C for 28 days. The combination of 10% and 20% Portland cement, sodium silicate, and NaOH, resulted in the strength of 41.1 MPa and 102.6 MPa, reflecting the effect of adding CaO to the mixture. Furthermore, Zhang et al. [11] used the metakaolin of an alkaline solution of NaOH and Na_2SiO_3 to stabilize a single mass with a low support capacity, in which the incorporation of the geopolymer showed a better mechanical performance than the theory of 15%, which was not stabilized or stabilized with cement Portland PC II. In another study, Rios et al. [12] demonstrated the stabilization of sandy silt for application as a sub-base layer for paving. The analyzed mixtures did not study the open use of lime, lime and sodium chloride, fly zinc and lime (as without sodium chloride), alkaline activated fly zinc with NaOH and Na_2SiO_3 and lime (as without sodium chloride), and also with cement, together with a commercial additive for the stabilization of soles destined for pavements. The authors evaluated the behavior, regarding the unconfined compressive, triaxial, and ultrasonic pulses for different healing times. The study did not make it clear that at the mixture of only lime, we do not reach the established compressive strength values, as for only flywheel lime, it is slightly above the lower limit of the standard of 3 MPa. A better performance was observed, using alkali-activated flywheel and lime, corresponding to approximately 5 MPa at seven days of curing and 9 MPa at 28 days, in contrast to 1 MPa obtained as Portland cement and additives.

The technique of soil stabilization has undoubtedly been widespread in the geotechnical engineering literature for years. Given the circumstance in which the available soil does not perform satisfactorily in the face of design requests, this alternative becomes necessary, since removing layers is unfeasible from an economic and environmental point of view. This way, stabilization acts as a resource capable of altering soil properties through mechanical, physical, chemical, and thermal treatments. The compaction in soils or soil-cement never manages to expel all of the air from the soil-water-air or soil-cement-water-air system. The strength cannot be correlated with the water/cement factor (w/c), as this only applies to materials where the air has been completely expelled, and the existing voids are filled with water, as is the case with traditional mortars and concrete.

The rational dosing methodology for cemented soil mixtures was established by Consoli et al. [13], similar to the water/cement (w/c) factor for concrete, which relates the volume of voids and the volume of the cementing agent. The dosage method was based on the unconfined compressive strength tests for Botucatu sandstone residual formation soil, stabilized with contents from 1% to 12% of Portland cement. This methodology obtains the porosity/volumetric cement content (η/C_{iv}) curve about the unconfined compressive strength, called the dosage curve. From this curve, it is possible to define the desired strength, according to the design requests, and then it is possible to obtain the volumetric content of the cement and the porosity necessary to achieve the target strength. The general equation to estimate the compressive strength was defined by Consoli et al. [13] as:

$$q_u = A\left[\eta/C_{iv}^{b}\right]^{-k} \tag{1}$$

where q_{u} is the compressive strength, η is the porosity, and A, b, and k are scalars dependent on the soil and cement properties.

Lemos et al. [14] conducted a laboratory and field study on the stabilization of organic clay with Portland cement. Among the main results, it was found that the final porosity of the specimens controlled the mechanical properties of the mixtures, with a notable increase in resistance concerning unstabilized soil. The authors also reported the decreased moisture and organic matter content after the curing period, due to interactions with the added cement. Horpibulsuk et al. [15] analyzed the effect of cement content on the development of unconfined compressive at seven days of curing in high-plasticity clay soil mixtures. The mixtures were compacted at the maximum dry apparent specific weights in the energy of the standard and modified Proctor test, with a constant moisture content. The study by Li et al. [16], when developing geopolymeric compounds from metakaolin and heat-treated clay, identified that the reaction products formed from these precursor materials are different, mainly due to the presence of cristobalite found in heat-treated clay. In this way, the crystalline phase referring to the sodium and calcium silicate mineral was evidenced by Sun et al. [17], when using ceramic residue from tiles and bricks as a precursor material for the alkaline activation. In addition, another material, such as silica fume, has been introduced to create geopolymers. It has been found that the strength and durability could be further increased if the negative effect of the higher amounts of silica fume on the geopolymerization retardation could be prevented [18].

The use of traditional materials for the improvement of low-capacity soils is widespread. However, it is known that the production process for obtaining Portland cement and hydrated lime demands a high energy consumption, exploitation of environmental resources, and the emission of gases of the greenhouse effect. This way, the search between the use of residues, which have potential characteristics, has been studied concerning soil improvement. For this reason, this study explores the development of a new geomaterial, based on roof tile residue, combined with soil and cement. The main objective of the research is to determine the effectiveness of the porosity-to-cement index on the split tensile, unconfined compressive, and microstructure of the compacted blends little explored in the current literature. The compacted blends were cured under 28 days, and the tests were carried out in saturated conditions to avoid the matric suction effect on the strength.

2. Materials and Methods

The first stage of the experimental program included the physical characterization tests of the soil, roof tile waste, and cement. ASTM D2487 [19], ASTM 4318 [20], ASTM D854 [21], and NBR 16605 [22] were applied, respectively, for the soil granulometry and crushed tile, Atterberg limits of the soil, specific gravity of the soil and roof tile waste, and the actual specific gravity of the grains of the cement. In the second stage, specimens were molded, cured, and subjected to unconfined compression and splitting tensile tests, according to the literature [23–25]. The materials' characteristics are specified in the following section.

2.1. Materials

Four materials were used in the present research: soil, roof tile waste, pozzolanic Portland cement (with CP II-Z nomenclature in Brazil), and water.

A demolished state in Fazenda Rio Grande, Brazil, was used as a sample collection site for a soil sample to carry out all characterizations and mechanical strength tests, avoiding contamination, and for the roof tile waste (waste residue class A [26] or waste code 170103 [27]), then subjected to a mechanical crushing process. CP II-Z is commercialized in Southern Brazil, mainly in Curitiba, and could be used to improve the local soils' mechanical properties, since it has the addition of pozzolanic material and a low hydration heat. Finally, for all laboratory procedures, distilled water at 25 ± 3 °C was used to limit the number of variables in the study and to avoid unwanted reactions (see Table 1).

Table 1. Physical properties, RT waste, and the sedimentary silty soil samples.

Physical Property of the Raw Material	Soil Results	RT Results
Liquid limit, %	53.0	-
Plastic index, %	21.4	Non-Plastic
Specific gravity	2.72	2.38
Fine gravel (4.75–19 mm), %	-	22.0
Coarse sand (2.0–4.75 mm), %	-	17.0
Medium sand (0.425–2.0 mm), %	7.45	12.0
Fine sand (0.075–0.425 mm), %	25.88	8.0
Silt (0.002–0.075 mm), %	57.59	29.0
Clay (diameter < 0.002 mm), %	9.08	12.0
Medium diameter (D_{50}), mm	0.0245	0.20
USCS Classification	MH	-

According to ASTM D2487 [28], the soil is classified as elastic silt with sand (MH). Table 1 shows the results of the soil and crushed roof tile characterization tests. X-ray spectroscopy (EDX) was used to identify the total quantitative chemical composition of the soil. Moreover, Table 2 shows the chemical composition of the soil samples. SiO_2, Al_2O_3, and Fe_2O_3, are found as expected in the residual and sedimentary soils and actively contribute to the chemical soil stabilization.

Table 2. Chemical composition of the soil sample.

Chemical Compost	Concentration by Weight (%)
SiO_2	52.22
Al_2O_3	23.15
Fe_2O_3	11.44
CaO	0.04
MgO	0.27
K_2O	0.38
Na_2O	0.03
TiO_2	1.29
MnO	0.19
P_2O_5	0.23
LOI	10.76

X-ray diffraction analysis (XRD) results of the roof tile waste sample was explored. The following mineral were detected: quartz (SiO_2), sericite [$KAl_2(AlSi_3O_{10})(OH)_2$], and hematite ($Fe_2O_3$) phases, in concordance to the study carried out by Baldovino et al. [1]. Tables 1 and 3 show the soil and cement characterization test results. It is to be noted that the largest soil size corresponds to 57.6% silt (0.002 mm < diameter < 0.075 mm) (Table 1). The specific gravity is 2.71 for the soil samples and 3.15 for the cement. Reddish pink is the predominant color of the soil due to the CaO oxidation and 10.48% presence of iron in a subtropical zone, as shown in Table 2. Finally, Table 3 reports the cement's chemical composition and physical properties.

Table 3. Physical and chemical composition of the Portland cement sample.

Property	Value
Al_2O_3 (%)	4.30
SiO_2 (%)	18.96
Fe_2O_3 (%)	2.95
CaO (%)	54.46
SO_3 (%)	2.54
MgO (%)	3.68
The insoluble residue (in %)	11.04
Axial resistance at seven days (MPa)	20.1
Axial resistance at 28 days (MPa)	41.2
The fineness of the cement particles (in %)	1.82
The density of the cement particles	3.15

2.2. Definition of the Porosity, Dry Unit Weights, RT, Cement, and Moisture Content

To define the molding points, according to the NBR 7182 [29], the soil compaction tests were carried out in three efforts: standard, intermediate, and modified, as presented in Figure 1. In accordance with Table 4, four molding (A1, A2, A3 and A4) points were established for the specimens. The mold points were strategically defined, simulating field conditions, especially pavements and shallow foundation reinforcements [30].

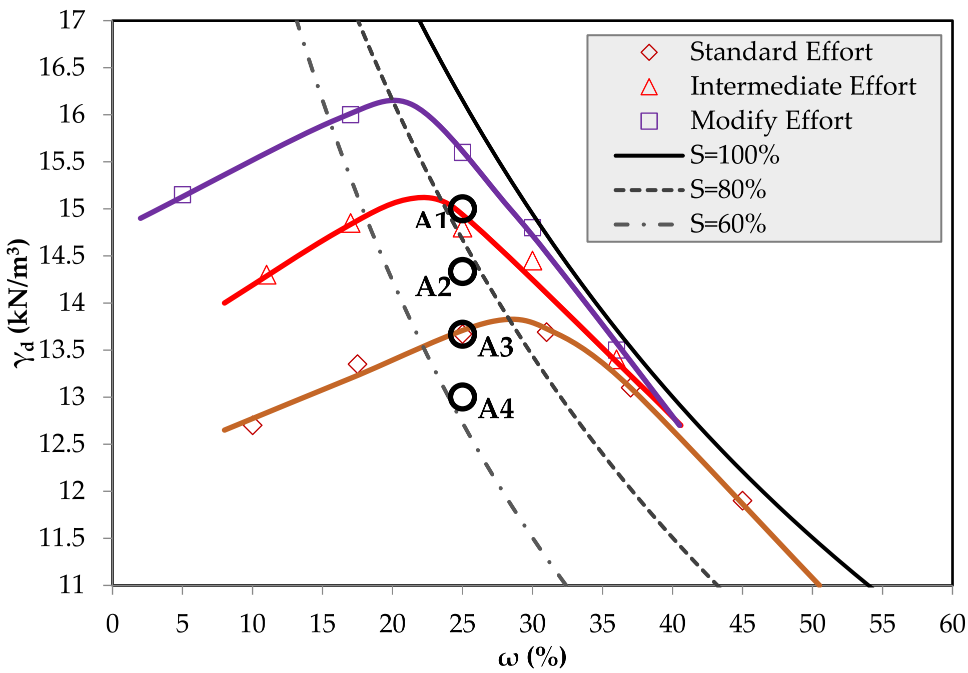

Figure 1. Results of the compaction curves of the soils and molding points (γ_d and moisture).

To choose the moisture content, it was decided to use the optimal moisture content descending from the intermediate energy compaction curve of the mixture of materials [see Figure 1]. Thus, the moisture content used in the mechanical analysis tests was set at the integer value of 25%. Likewise, the dry apparent specific weight adopted was the dry apparent specific weight obtained from the same straight line at 25% humidity, between

13 and 15 kN/m^3 (adding 0.67 kN/m^3). This same methodology was used by Baldovino et al. [31] to study the soil-cement mixtures. Other authors (e.g., [32–34]) have also used this methodology to study soil-cement mixtures and activated materials with residues. Considering the previous studies [8,9,35–37], the percentages of RT chosen were: 5, 15 and 30%. These percentages were combined with 3, 6, and 9% Portland cement.

Table 4. Molding points.

Molding Point	ω	γ_d (kN/m^3)	Saturation Degree
A1	0.25	15.0	0.85
A2	0.25	14.3	0.77
A3	0.25	13.7	0.70
A4	0.25	13.0	0.64

2.3. Preparing the Specimens for the q_u and q_t Tests

The porosity values of the compacted blends, controlled from dry unit weights (γ_d) and molding moistures, were defined, based on the soil and soil compaction curves with the addition of glass powder and carbide lime, presented in Figure 1. The curves defined the γ_d values between 13 kN/m^3 and 15 kN/m^3 and the molding moisture contents of 25%, were defined.

Specimens 100 mm high and 50 mm in diameter were molded for the splitting tensile and unconfined compression tests. The specimens were prepared through weighing, mixing, static compaction, packaging, storage in a wet chamber, and curing. The materials (soil, RT, lime, and cement) were weighed on a scale with a 0.01 g sensibility. The fraction of the soil used was dried and passed through the #10 mesh sieve (diameter < 0.149 mm). The RT and the cement were mixed with the soil with a spatula until the mixture was uniform. Then, water was added, continuing the mixing process until a visibly homogeneous material was obtained. The total dry mass of the samples is composed of the sum of the dry mass of soil, ground RT, and cement, when these are added. In this way, the amounts of each additive added, and the moisture content is determined, in relation to the total dry mass of each specimen. The total amount of the mixture allows the molding of the specimens in triplicate, with a small amount of soil left over, to determine the moisture content to reach 25%.

Once mixed, the amount of material needed to produce a specimen is divided into three equal parts. These are kept in containers with lids to avoid moisture loss until the moment of compaction. At the end of this procedure, two samples of the material are taken and placed in capsules. These are taken to the oven for drying and the subsequent determination of the moisture content. The moisture content of the specimen is defined as the average of the two determined moisture contents.

The specimens were compacted into three layers, then, the material was weighed for each layer and separated into containers with lids (to mitigate moisture loss). With the leftover material, the capsules were weighed to check the moisture content. Then, the process of molding the specimens began. Scarification between the intermediate layers (first and second layers) was carried out to achieve a more outstanding adhesion. The forms of the specimens were lubricated with a release agent (mineral or synthetic and of low viscosity) to facilitate extrusion and, thus, to prevent the specimen from "sticking" to the formwork. Following the extrusion, the specimen was weighed and, with a digital caliper, its dimensions were measured (the diameter was measured at the base, in the middle, and at the top; and the height was measured in three directions; the simple arithmetic mean, taken for the diameter and height). The specimen was immediately placed in an airtight bag to avoid variations in the moisture content and was stored in a specific warehouse in the laboratory. The specimens were considered suitable for testing if they met the following criteria: degree of compaction $\pm$ 1% of the target value; moisture content $\pm$ 0.5% of the target value; diameter $\pm$ 1% of the target value; and height $\pm$ 2% of the target value; and both never larger than 2 mm.

During the curing period (i.e., 28 days), the specimens cured at a temperature of 23 ºC (± 3 °C), were placed in a humid chamber with a relative humidity of approximately 95%. The samples, after being cured, were then submerged in a container with water for a period of 24 h, to approach the saturation condition and avoid the incidence of suction in the mechanical behavior of the improved soil. Although the suction is not removed, it is reduced. Immediately before the compression and the split tensile test, the samples were removed from the tank and superficially dried with an absorbent tissue. As an evaluation criterion for the test, it is stipulated that the individual resistances of the three test bodies should not exceed more than 10% of the average resistance of the whole.

The unconfined compressive and tensile tests were performed in an automatic press with a resolution of 2.5 N force and 0.01 mm deformation. The speed of both tests was 1 mm per minute. The procedures of the unconfined compression tests followed the ASTM D2166-03 [38]. In addition, the split tensile strength tests adhered to the Brazilian standard NBR 7222 [39]. In total, 216 specimens were used in this research for the compressive and tensile tests. Since the tests were performed in triplicate and four dry unit weights were used, for example, the 3% cement + 5% roof tile mix was compacted 24 specimens (for q_t and q_u measurements). Because nine mixes were made (i.e., 3% cement + 5% roof tile, 3% cement + 15% roof tile, 3% cement + 30% roof tile, 6% cement + 5% roof tile, 6% cement + 15% roof tile, 6% cement + 30% roof tile, 9% cement + 5% roof tile, 9% cement + 15% roof tile, and 9% cement + 30% roof tile), a total of 216 specimens were prepared.

2.4. Chemical Microanalysis and EDX Tests

The SEM technique is based on the premise that when an electron beam interacts with the surface of a sample, various types of electrons are generated, such as secondary and back-scattered electrons, that can be captured to create an image of the surface features and composition of this. The data is collected by scanning the electrons emitted by the sample, which then provides an image that can reflect the topography of the sample or its composition. The technique can be complemented with an EDX device to study the chemical composition in a strategic area or point.

An Oxford (Penta FET125 Precision) X-ACT and micro-mass analyses, using a laser micro-mass analyzer (LAMMA-1000, model X-ACT) and type X-ray energy dispersion spectrometer were used. The samples (Soil + 6% Cement + 15% RT) previously subjected to curing and unconfined compressive and split tensile testing of the reactions after 28 days of curing, were polished by the wet method with ethanol to avoid the material reactions until obtaining a sufficiently smooth surface that allows the reliability of the compositional analysis. Finally, the samples were vacuum dried and metalized with gold for the subsequent analysis by microscopy. The compositional analyzes with EDX were performed on some points of samples.

3. Optimization and Design Parameters for Determining and Estimating the Strength

The void volume and cement volume were considered as two parameters of the tested specimens and control molding to estimate the unconfined compressive strength and split tensile strength of the artificially cemented soil with cement and RT additions. As mentioned in Baldovino et al. [1] the initial porosity (η) of the mixes depends on the cement and the RT grains, cement content (*C*), the dry unit weight of the mix (γ_d), and the unit weight of the soil (γ_{ss}, $\gamma_{sc,}$ and γ_{SRT}). In addition, the cement volume is represented by the volumetric cement content (C_{iv}), while η/C_{iv} represents the porosity/volumetric cement content index (η/C_{iv}), introduced in the literature by Consoli et al. [13], based on previous studies [40]. According to Equation (2), the strength of the cement-stabilized soils could be calculated as a function of η/C_{iv}.

$$q_u \vee q_t = A_q\,[\eta/C_{iv}^{b}]^{-k} \tag{2}$$

Henzinger et al. [24] have established correlation functions that allow relating the initial porosity of the compacted mixture (η) and the volumetric content of the added cement (C_{iv}), with the compressive strength and other mechanical properties of various types of soils, stabilized with cement. These formulations, of an empirical nature, have made it possible to establish a rational dosage method. Previously, Equation (2) was thought to be purely empirical. Nevertheless, recently Diambra et al. [23,41], through a mathematical model, assuming that the failure resistance of the soil (through the theory of the critical state of soils) and of the reaction products of the cement with the water in the soil or cementitious matrix (through the Drucker–Prager failure criterion) overlap, it was found that these formulations are not purely empirical, showing that k and b exponents depend mainly on the parameters related to the soil matrix and that the value of k is close to the inverse of the value of b, and the magnitude of the scalar A_q is the result of the joint properties of the soil and the cementitious matrix. For the fine soils, it is expected to be a good fit with the index using an exponent (b), close to 0.28, is commonly used with a good fit for soils of this type, while for granular soils, this value is close to unity. The physical meaning of this internal exponent is that the greater it will be, the more the soil is ligand-dependent for the reaction development. From the choice of the exponent (k) by an iteration process of fitting the curves, the power equation's external fitting exponents (b) are determined.

In general, the parameter η/C_{iv}^{b} makes it possible to reconcile the effects of porosity (η) and the volumetric content of cement (C_{iv}) on the unconfined compressive and split tensile strengths, allowing the mutual compensation between these parameters to maintain constant the value of q_u or q_t, through different values that the exponent b can assume. If the effect of porosity is greater than the cement content, the value of b is less than 1.0; otherwise, b is more significant than 1.0. Additionally, if the effect of both parameters is equal, the value of b takes the value of 1.0. The exponent k corresponds to a polynomial fit, and A_q is a scalar.

To optimize the split tensile and unconfined compressive strength prediction of all cement-soil-RT compacted blends, the criterion η/C_{iv}^{b} was used. Since b is a function of k, both exponents have a constant relationship. One way to correlate them is by applying a constant "b_o" that multiplies k, i.e., $b = b_o k$, where "b_o" is also dimensionless. Thus, a new formula for q_t and q_u was proposed as a function of η, C_{iv}, b_o, and k parameters, as shown by Equation (3).

$$q_u \vee q_t = A_q \left[\frac{\eta}{(C_{iv})^{b_o k}} \right]^{-k} \tag{3}$$

The values of porosity η and volumetric cement content C_{iv} are pre-established values for each cement-RT-soil specimen through weight-volume relationships [using Equation (4)], so the values of b_o and k must be calculated. For calculating the parameters b_o and k, a simple optimization was used, considering the molding conditions of each specimen and its respective split tensile or unconfined compressive, as shown in Equation (4):

$$q_u \vee q_t = A_q \left[\frac{\eta}{(C_{iv})^{b_o k}} \right]^{-k} = A_q \left\{ \frac{100 - 100\left(\frac{\gamma_d}{1+C+RT}\right)\left(\frac{1}{G_{SS}} + \frac{C}{G_{SC}} + \frac{RT}{G_{SRT}}\right)}{\left[\left(\frac{\gamma_d}{1+C+RT}\right)\frac{C}{G_{SC}}\right]^{b_o k}} \right\}^{-k} \tag{4}$$

where Gss, Gsc and G_{SRT} are the specific gravity of the soil, cement, and RT grains, respectively. The coefficient of determination (R^2) of each molding condition (i.e., depending on the RT waste and strength test) was chosen to optimize the prediction of q_u and q_t equations, depending on the η/C_{iv}^{b} criterium. Using exponents of adjustments b_o and k helps to improve the behavior of the experimental points of the split tensile and unconfined compression. So, the optimization of q_u was made using the R^2 as the main parameter, given as:

$$R^2 = 1 - \left(\frac{\Sigma\left(q_u - q_{u(i)}\right)^2}{\Sigma\left(q_u - \overline{q_u}\right)^2} \right) \tag{5}$$

where q_u is the experimental unconfined compressive strength of each soil-cement-RT sample, $q_{u(i)}$ is the theoretical or calculated unconfined compression to each sample and $\overline{q_u}$ is the average unconfined compressive strength of all experimental samples. The optimization of the q_t was also conducted through the R^2 calculation, as shown by Equation (6):

$$R^2 = 1 - \left(\frac{\Sigma\left(q_t - q_{t(i)}\right)^2}{\Sigma\left(q_t - \overline{q_t}\right)^2} \right) \quad (6)$$

where q_t is the experimental split tensile strength to each specimen, $q_{t(i)}$ is the theoretical split tensile to each soil-cement-RT sample and $\overline{q_t}$ is the average split tensile of all experimental samples. The mean absolute percentage error (MAPE) was employed to verify the R^2 values in each optimization process. During the optimization process of coefficient and the MAPE calculation, the factor b_o was considered an independent variable, while parameters k and A_q were considered dependent variables. In turn, the pair composed of b_o and k was taken as the direct influence of the value of A_q. Thus, Equation (4) shows the extended optimized expression for any molding condition, depending on the materials' physical properties of sedimentary soil, cement, and RT used in the present research.

4. Analysis of the Laboratory Data and Discussions

4.1. Influence of the Porosity-to-Volumetric Cement Content Index (η/C_{iv}) on the Unconfined Compressive and Splitting Tensile Strength, Using the Optimized Parameters b_o and k

Figures 2–4 show the influence of the porosity-to-volumetric cement content index (η/C_{iv}) on q_u and q_t for 5, 15 and 30% roof tile residue, respectively, for the optimized parameters of b_o = 0.066 and k = 4.37, obtained by applying Equations (4)–(6) on the data of all of the specimens. The relation η/C_{iv} adjusted to the value $b = b_o k = 2.9$ directly influences the q_t and q_u values of the soil-cement-RT mixtures. The volumetric cement content is the cement volume divided by the specimen volume (198.35 cm^3). Note that a decrease in the η/C_{iv} ratio increases the strength value due to a decrease in voids and the corresponding increase in the dry unit weight of the samples, as shown in Figure 5a. It follows that, similarly to the cement content, the compacted mixture's porosity strongly influenced the simple compressive strength of the tailings cement. Regardless of the cement content used, a decrease in the material's porosity promoted considerable gains in strength, due to a more significant number of contacts between particles and a more outstanding interlocking between the soil particles. In addition, the more remarkable ability to distribute the stresses inside the specimen and the greater ability to mobilize friction in lower porosity states, contribute to the gain in the compressive strength of the RT-cement mixture.

The increase in the dry unit weight of the samples (defined in Table 4) is a function of the increase in the cement content of specimens. For 5% rood tile addition, the value of η/C_{iv} ranged from 11.94 to 44.87 (Figure 2). For 15%, it ranged from 12.80 to 48.26 (Figure 3), and for samples with 30% tile, the η/C_{iv} ratio varied between 14.11 and 54.08 (Figure 4). Thus, the ranges are 32.96, 35.46, and 39.97 for 5, 15, and 30% RT. The range of η/C_{iv} increases with the increased RT content because, with the increasing tile content, the specific gravity of the roof tile contained in the samples is smaller than that of the cement and the soil, which increases its porosity, as shown in Figure 5b.

The potential increasing relationship between $\eta/C_{iv}{}^b$—q_u and $\eta/C_{iv}{}^b$—q_t with the decrease of $\eta/C_{iv}{}^b$ is limited to the percentages of cement and dry unit weights used in this study. A η/C_{iv} ratio/index close to zero can result in infinite resistances. Moreover, a η/C_{iv} index near infinity can result in null relations. Other limitations on the ratio η/C_{iv} must be mentioned, such as the type and amount of the binder to stabilize the soils. The excessive use of the binder can sometimes decrease the mechanical resistance of the mixtures, such as soil-lime and soil-ash, as already reported in the literature by Meurant [42]. With this, the value of η/B_{iv} for a constant value of γ_d and with the increase, B_{iv} may result in a decrease in q_u and q_t. These limitations when $\eta/C_{iv}\rightarrow 0$, $\eta/C_{iv}\rightarrow\infty$, and η/B_{iv} for the high values of

B_{iv} have not yet been reported in the literature, so this study is focused on the values for η/C_{iv} reported here, which, according to Figures 2–4, vary from 30 and 50%, which would be close to field conditions, depending on project specifications.

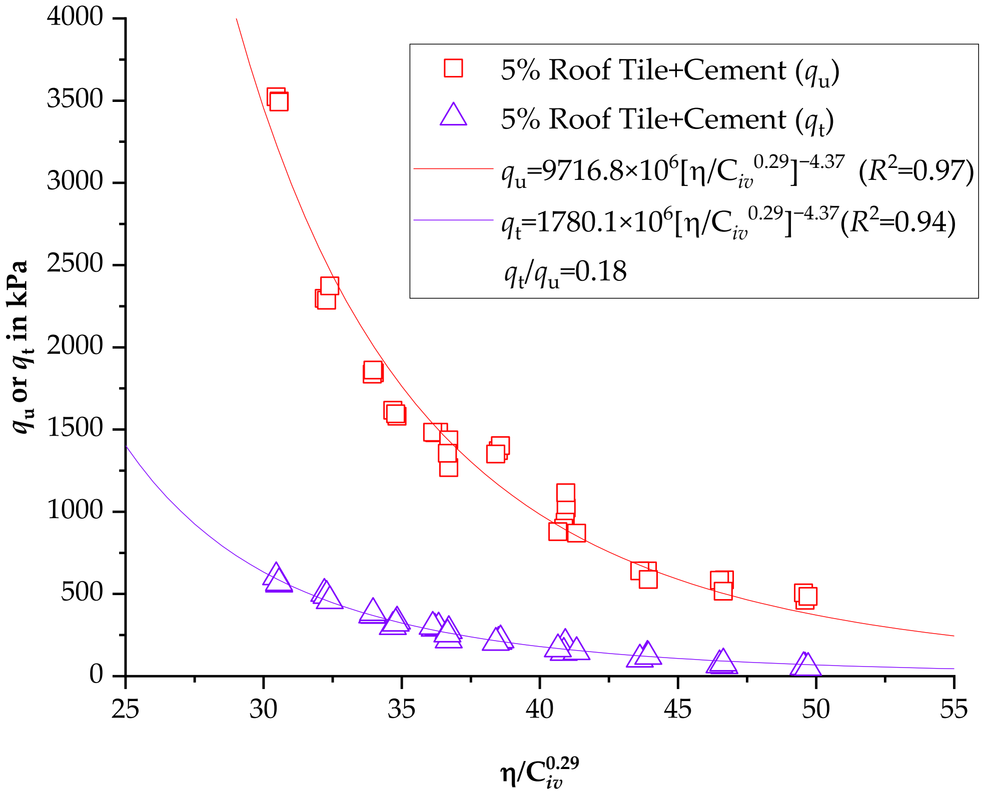

Figure 2. Variation of q_u and q_t with the porosity/volumetric cement ratio (using the exponent b = 0.29) for 5% of the roof tile waste.

With the above analysis, several postulates can be mentioned from the results shown in Figures 2–4:

- There is an increase in q_u and q_t with the increase in the cement percentage and with the increase of the dry unit weight of the molding, defined in Table 4;
- Since there is a fall of q_u and q_t as a function of RT, Figures 2–4 also show this decrease as a function of the percentages RT = 5% (Figure 2), RT = 15% (Figure 3) and RT = 30% (Figure 4), where the constant A_q decreases both for q_u and for q_t with the increase of RT. The value of A_q decreases by 8% from 5 to 30% of RT in the compression tests. For the tensile tests, the decrease in A_q was 12% from 5 to 30% of RT.
- Although A_q, q_u, and q_t decrease from 5 to 30% of RT, reusing the tile residue is vital. It is essential to reduce and reuse the volume of waste discarded from civil construction. Reusing this type of waste (RT) is intended to extend a product's life on civil constructions: in pavements, for example. Products in this category must indicate how many production cycles they can pass without affecting their main characteristics.

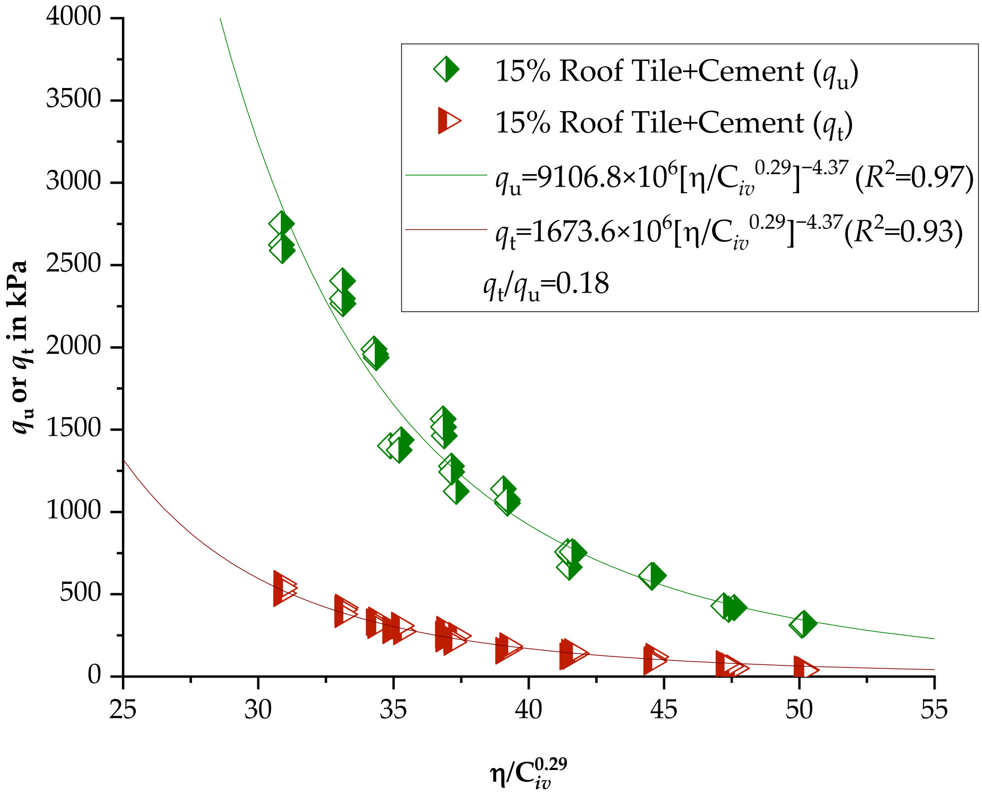

Figure 3. Variation of q_u and q_t with the porosity/volumetric cement ratio (using the exponent b = 0.29) for 15% of roof tile waste.

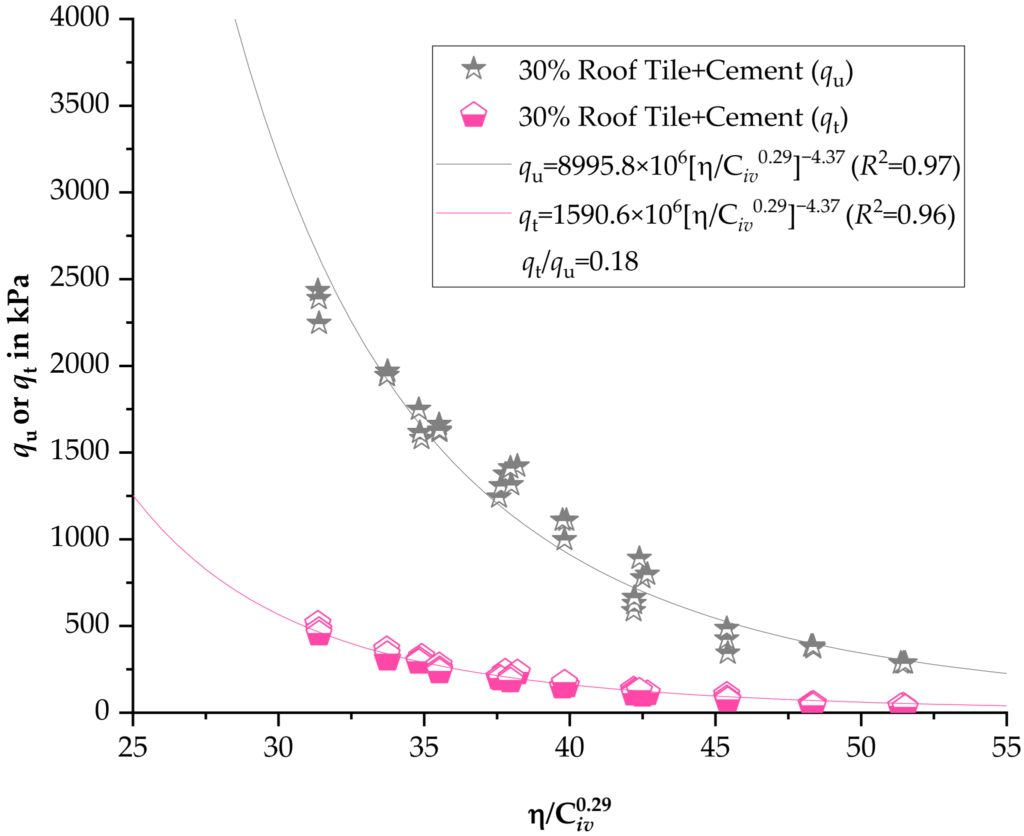

Figure 4. Variation of q_u and q_t with the porosity/volumetric cement ratio (using the exponent b = 0.29) for 30% of roof tile waste.

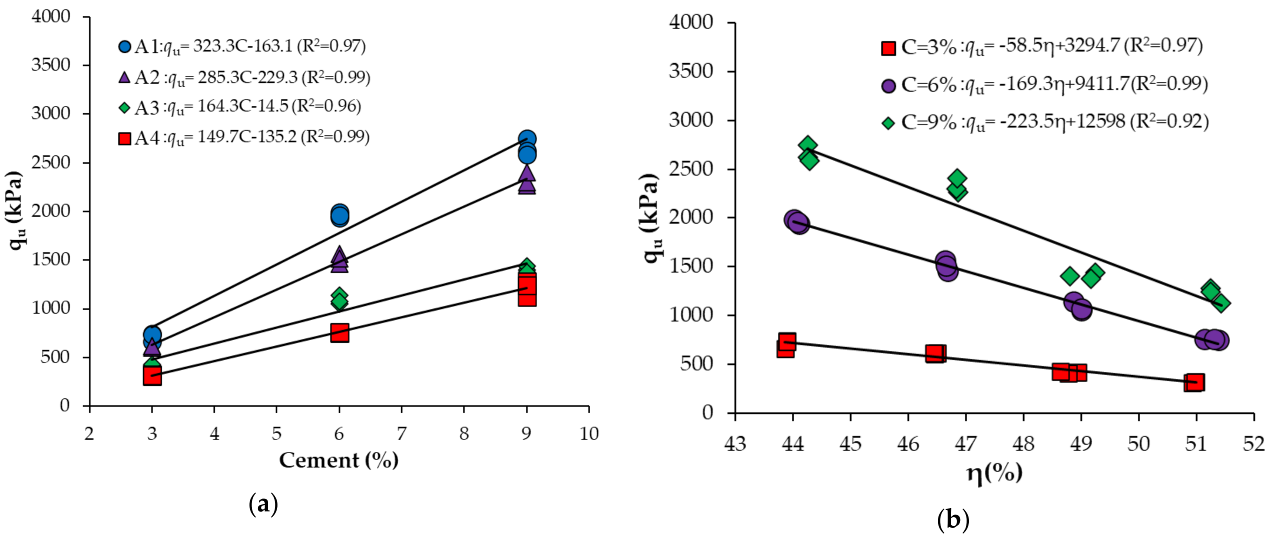

Figure 5. (**a**) Influence of cement percentages on the q_u for 15% roof tile waste; and (**b**) Influence of the porosity on the q_u for 15% roof tile waste.

The mixtures of soil-cement studied by Horpibulsuk et al. [15] were compacted at the maximum dry densities of the standard and modified Proctor tests, with a constant water content (optimal humidity). The study concludes with the importance of the compaction energy in the development of strength (the higher the compaction density, the greater the resistance) and defines three zones, based on the content of added cement. An active zone, for cement percentages less than 11%, where the increase in cement content is associated with a significant increase in strength. An inert zone, for added cement percentages between 11 and 30%, where the most substantial growth rate is low, with respect to the added cement content; and finally, a zone of deterioration, where the resistance decreases with the increase in the percentage of added cement, for percentages greater than 30% of cement. Thus, in the present study, the behavior of the soil-cement mixtures was similar.

4.2. Empirical Relationships between q_u and q_t

For each RT (in %), an empirical relationship between tensile/compression can be calculated as a function of η/C_{iv} directly. As the equations $q_u \vee q_t = A_q\left[\eta/C_{iv}^b\right]^{-k}$ have the same format (with a difference in the constants A_q, which can be divided into A_{qu} for compression and A_{qt} for tensile), when dividing $A_{qt}\left[\eta/C_{iv}^b\right]^{-k}$ and $A_{qu}\left[\eta/C_{iv}^b\right]^{-k}$, a constant is obtained (named ξ) that is equal to $\xi = A_{qt}/A_{qu}$ and independent of $\left[\eta/C_{iv}^b\right]^{-k}$. Thus, from Figures 2–4 the empirical relationships for 5, 15, and 30% of RT can be calculated. Equations (7)–(9) show the q_t/q_u ratios for 5, 15, and 30% of RT, respectively. The calculations of q_t/q_u can also be seen in Figures 2–4.

$$\xi = \frac{q_t}{q_u} = \frac{1780.1 \times 10^6 \left[\eta/(C_{iv})^{0.29}\right]^{-4.37}}{9716.8 \times 10^6 \left[\eta/(C_{iv})^{0.29}\right]^{-4.37}} = 0.18 \quad (7)$$

$$\xi = \frac{q_t}{q_u} = \frac{1673.6 \times 10^6 \left[\eta/(C_{iv})^{0.29}\right]^{-4.37}}{9106.8 \times 10^6 \left[\eta/(C_{iv})^{0.29}\right]^{-4.37}} = 0.18 \quad (8)$$

$$\xi = \frac{q_t}{q_u} = \frac{1590.6 \times 10^6 \left[\eta/(C_{iv})^{0.29}\right]^{-4.37}}{8995.8 \times 10^6 \left[\eta/(C_{iv})^{0.29}\right]^{-4.37}} = 0.18 \quad (9)$$

The correlation established between the tensile/compression was demonstrated by Consoli et al. [43], and Consoli [44] as the ratio between the tensile strength and the simple compressive strength ($\xi = q_t/q_u$), in which the value found was 0.15 for mixtures of sandy soil with Portland cement. A range of similar values was found for different materials, as in Consoli et al. [45], when studying mixtures of milled asphalt material (RAP) stabilized with glass powder and carbide lime, obtaining a ratio of 0.15. Scheuermann et al. [46] studied the behavior of a dispersive and sulfated soil stabilized with carbide lime and reinforced with glass fibers and found the ratio $\xi = q_t/q_u$ of 0.18. Regarding the recent use of alkali-activated binders for the soil stabilization, Dos Santos et al. [47] obtained a ratio of 0.20.

Since both the external exponent and the internal exponent (−4.37 and 0.29) are made compatible, the ratio shown by Equations (7)–(9) is based on the scalar A, verifying that there is a proportionality between these tests, which is independent of porosity, the volumetric content of the cementing agent, therefore, independent of the $\jmath/(C_{iv})^{0.29}$ index for the variables studied here. That is, the ratio $\xi = q_t/q_u$ found means that the value of the tensile strength by the diametral compression is equivalent to 15% or 16% of the simple compressive strength, evidenced through the curves in Figure 6 and corroborated by the results previously found in the literature.

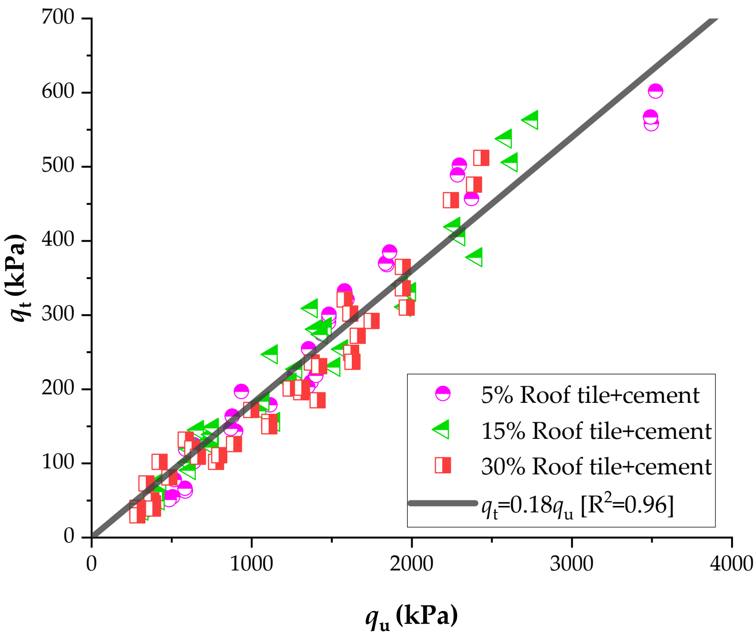

Figure 6. Direct empirical relationship between the tensile and compressive strength for all specimens' tests, using different dry unit weights, cement content and roof tile waste.

The correlation coefficient obtained was $R^2 = 0.96$, which indicates an excellent correlation between the results exposed here through a linear trend. Therefore, it is possible to validate the rational dosage methodology through the $\eta/(C_{iv})^{0.29}$ index through tests of unconfined compressive strength or split tensile strength since these tests are closely related.

4.3. Dosage Equations for Estimating and Predicting the Strength of Roof Tile-Soil Mixes with Cement

A dosage equation can be proposed to estimate the value of splitting the tensile and unconfined compressive strength for any cement and roof tile content in the ranges of the present research (from 3 to 9% for cement and from 5 to 30% for tile) with the use of the ratio $(\eta/C_{iv}{}^{0.29})^{-4.37}$. If the value of A_q in Equations (7)–(9) is divided by $10^6(\eta/C_{iv}{}^{0.2})^{-4.37}$, the constants of 9716.8, 9106.8, and 8995.8 kPa for 5, 15, and 30% RT, are obtained for q_u. For q_t, the constants of 1780.1, 1673.6, and 1590.6 kPa are obtained for 5, 15, and 30% of RT, respectively. If the points [for q_u: (9716.8 kPa, 5%), (9106.8 kPa, 15%) and (8995.8 kPa, 30%); and for q_t: (1780.1 kPa, 5%), (1673.6 kPa, 15%) and (1590.6 kPa, 30%)] are plotted in the same Cartesian plane, a potential tendency ($R^2 = 0.99$ for q_t and $R^2 = 0.95$ for q_u, respectively), are obtained, as shown in Figure 7. The dosages expressions of the mixtures for the compressive and tensile strengths are shown in Equations (10) and (11), respectively.

$$q_{\mathrm{u}} = 10,392 \times 10^6 (\mathrm{RT})^{-0.044} \left(\eta / C_{iv}^{0.29}\right)^{-4.37} \quad (10)$$

$$q_{\mathrm{t}} = 1971 \times 10^6 (\mathrm{RT})^{-0.062} \left(\eta / C_{iv}^{0.29}\right)^{-4.37} \quad (11)$$

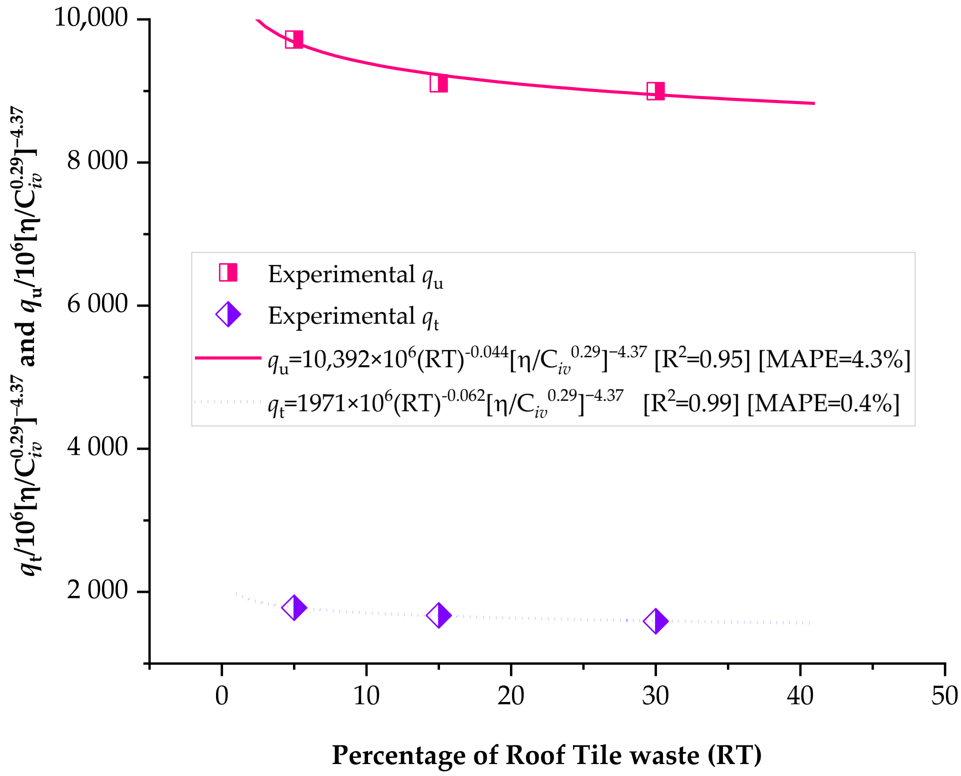

Figure 7. Estimate q_{u} for any cement content and roof tile waste content using the η/C_{iv} ratio (with b = 0.29 exponent) and the simple normalization resistances divided by 10^6 $[\eta/C_{iv}{}^{0.29}]^{-4.37}$.

The values of porosity and volumetric cement content of 216 specimens of the present study were inserted in Dosages Equations (10) and (11) for validation. The exponential curve's determination coefficient (R2) was 97% (Figure 8). Therefore, the $\eta/C_{iv}{}^{0.29}$ ratio is considered valid to estimate the soil-cement-roof tile waste mixtures of the present study. According to the literature, Consoli et al. [32] and Al-Subari and Ekinci [48], it is possible to obtain a unique ratio to determine the strength of the clayey and silty soils mixed with Portland cement. Furthermore, the present research established a single ratio by dividing the form q_{u} and $q_{\mathrm{t}} = A_{\mathrm{q}}(\eta/C_{iv}{}^{\mathrm{b}})^{-\mathrm{k}}$ by an arbitrary specific value of the splitting tensile and unconfined compressive strength, corresponding to a value of a given adjusted porosity, $\eta/C_{iv}{}^{\mathrm{b}} = \Omega$ (Equation (12)).

$$\frac{q_t}{q_{t-norm}\left(\frac{\eta}{C_{iv}{}^{b}} = \Omega\right)} \vee \frac{q_u}{q_{u-norm}\left(\frac{\eta}{C_{iv}{}^{b}} = \Omega\right)} = \frac{A_q\left(\eta/C_{iv}{}^{b}\right)^{-\mathrm{k}}}{A_q(\Omega)^{-\mathrm{k}}} = (\Omega)^{\mathrm{k}}\left(\eta/C_{iv}{}^{b}\right)^{-\mathrm{k}} \quad (12)$$

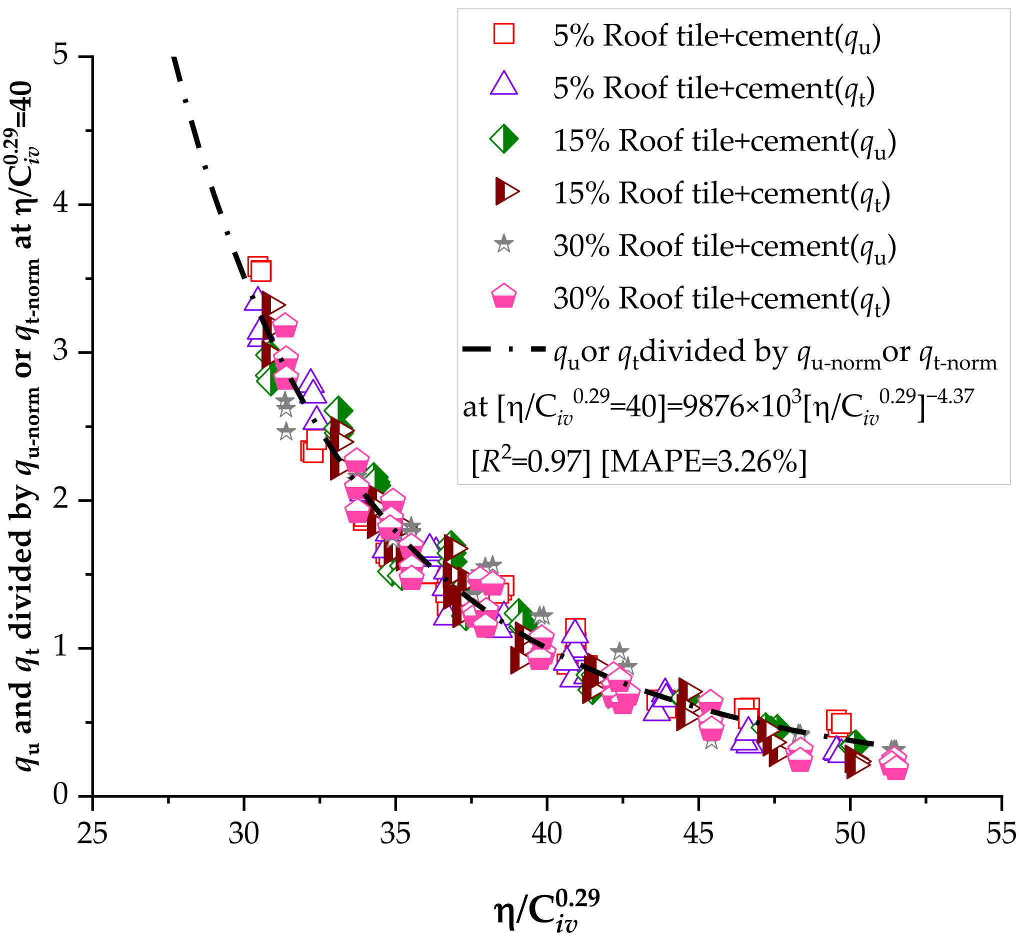

Figure 8. Normalization of the unconfined compressive and split tensile strength (for the whole range of $\eta/C_{iv}^{0.29}$) by dividing for q_u and q_t at porosity/cement index equal to 40%, considering the strength of the cement-treated silty soil-roof tile waste mixtures.

The Ω value of the present study was set to 40, due to the mathematical approximations of Figures 2–4. In the same manner that b = 0.29 and k = 4.37 were taken. Thus, the specific experimental q_u and q_t values of the 36 samples with 5% tile are divided by the A_q value of Equation (7), the specific q_u value of the 36 samples with 15% tile is divided by the A_q value of Equation (8), and for the 36 samples with 30% tile, the experimental q_u value is divided by the A_q value of Equation (9). This process of division is defined as the normalization of the strengths.

The normalization of the strengths was conducted in concordance with the literature [49]. Thus, for the tensile data, the same process can be made. The quotients obtained in these mathematical operations form a potential trend with a coefficient of determination of 0.97 and MAPE = 3.26%, described by Equation (13). Thus, Figure 8 presents the normalization of the strengths of the test specimens and their tendency, described by Equation (13) for the q_u and q_t data. Equation (13) can be compared with the lime-soil mixes, using the same soil [this study was reported by Baldovino et al. [50] for a Ω = 35 value. Figure 9 presents a comparative study with the normalized Equation for estimating the cement-soil-RT and lime-soil strengths, depending on the porosity/cement and porosity/lime index [η/L_{iv} (adjusted to b = 0.20 and k = 4.39)], respectively. It is noted that the mixtures using residue (from roof tile) and cement, reached higher resistances, compared to lime for the same porosity/binder index (η/B_{iv}) values. Thus, the efficiency of using the mixtures studied in this article (from the point of view of the resistance) is more apt to apply than those of the lime soil.

$$\frac{q_t}{q_{t-norm}\left(\eta/C_{iv}^{0.29} = 40\right)} \vee \frac{q_u}{q_{u-norm}\left(\eta/C_{iv}^{0.29} = 40\right)} = 9876 \times 10^3 \left(\eta/C_{iv}^{0.29}\right)^{-4.37} \quad (13)$$

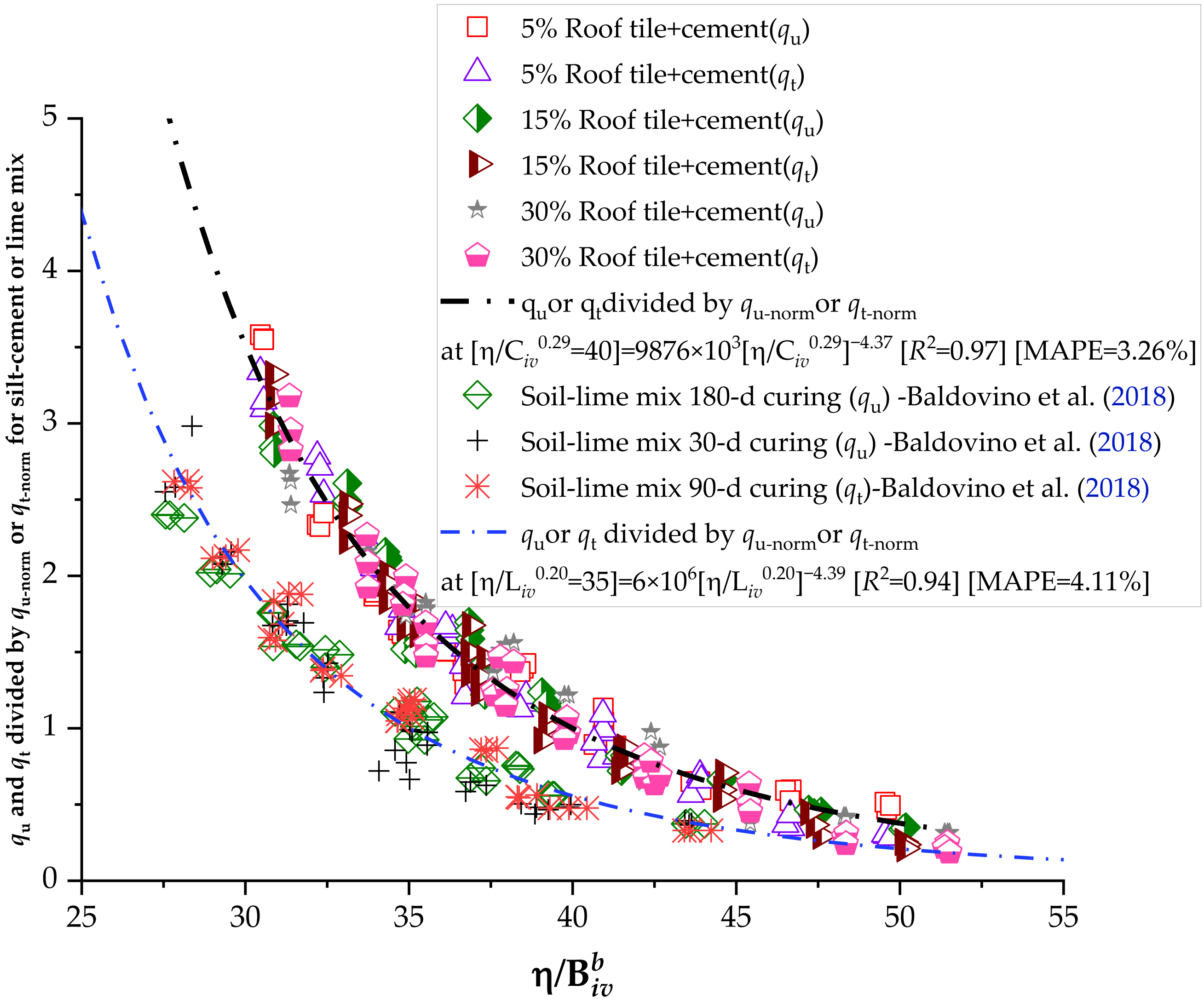

Figure 9. Normalization of the unconfined compressive and splitting tensile strength (for the whole range of porosity/cement index-adjusted to 0.29 exponent) by dividing for q_u and q_t at porosity/cement = 40, considering the strength of the cement-treated silty soil-roof tile waste mixtures; and the normalization of strength (for the whole range of porosity/lime index-adjusted to the 0.20 exponent) by dividing for q_u and q_t at porosity/lime = 35, considering the strength of the dolomitic hydrated lime-treated silty soil, reported by Baldovino et al. [50].

The tests with soil stabilized with cement and RT revealed the following: the increase in the cementation rates, the decrease in the initial moisture contents of the specimens and the use of RT in the moldings, reverberate, in general, in increases in the strengths of the q_u and q_t mixtures. The stress-strain behavior of the mixtures under undrained conditions was typical of cemented materials. It was proved that cement's porosity/volumetric content (η/C_{iv}) is adequate to predict the mechanical behavior of the RT-soil-cement mixtures, considering the parameters studied. It was verified that there is a direct proportionality between the tensile and compressive strengths of the mixtures, which is independent of the η/C_{iv} ratio, which is given through a single scalar ξ = 0.18.

4.4. Chemical Microanalysis Results

The chemical composition of the new geo-material formation was tested by EDX microanalysis, is presented in Figure 10 and Table 5. The content of each chemical element in the area (Figure 10) located in the glassy-like morphology, largely corresponds with the results of the XRF and DRX analyses (Tables 2 and 3) of the raw materials. The microanalysis results demonstrate a significant level of typical heterogeneity of the raw materials and the no-formation of new minerals, due to the absence of amorphous elements and the moderate cure temperature of the mixtures (25 °C).

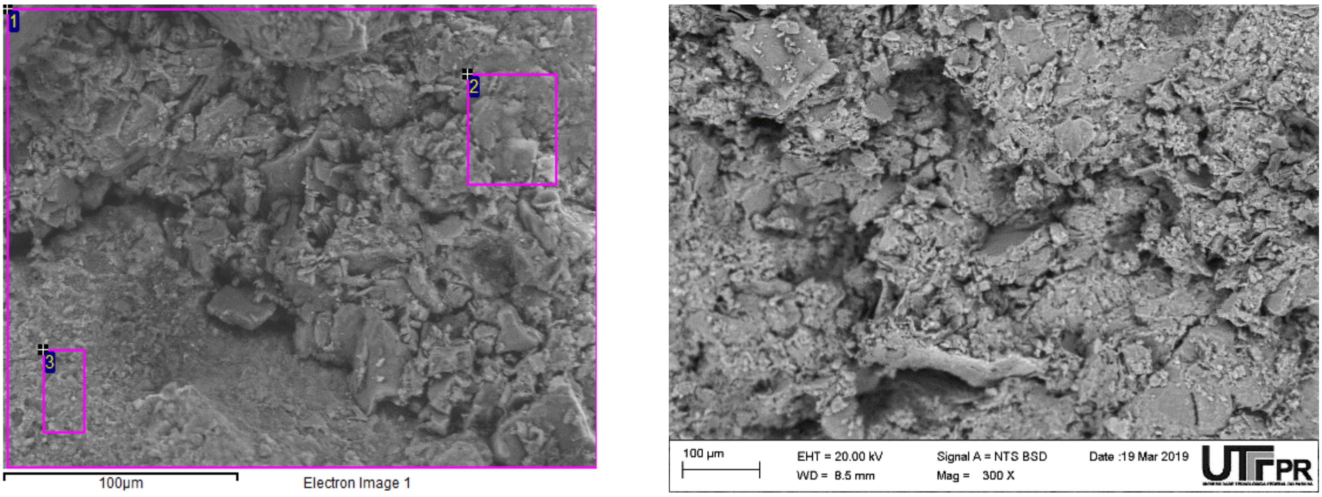

(**a**) (**b**)

Figure 10. (**a**) Area positions of the EDX analyses (results in Table 5). (**b**) MEV of soil-cement-RT.

Table 5. Chemical compositions (by EDX method) of the area for S+6%C+15%RT mix after 28 days of curing (see Figure 10).

Spectrum/Area	Chemical Compositions (wt.%)							
	C	O	Al	Si	K	Ca	Ti	Fe
1	-	65.25	13.40	15.87	0.30	1.59	0.51	3.07
2	8.36	60.79	13.18	13.52	0.25	0.39	0.66	2.85
3	12.66	60.61	8.05	11.24	0.21	5.80	0.20	1.22
Maximum value	12.66	65.25	13.40	15.87	0.30	5.80	0.66	3.07
Minimum value	8.36	60.61	8.05	11.24	0.21	0.39	0.20	1.22

Figure 10 demonstrates a detailed comparison of the SEM images for the 300x approximation, where the presence of the C-A-S-H reaction product can be visualized at several points of the image, marked in one as an example, due to the high presence of the C-A-S-H gel and sample homogeneity. The C-A-S-H gel is a typical pozzolanic cement product due to the reaction between the reactive calcium of the lime and the aluminum silicates. The C-S-H gel was also verified, with the structure in the traditional beehive form. The C-S-H phase detected tobermorite-like structures formed during the hydration processes of Portland cement [51].

As illustrated in the SEM images of Figure 10, the clay particles had edges, and their structure contained a good number of small voids. With the treatment with cement and RT, some clay particles were coated with cement, and a smaller number of voids/pores were observed. Compared to the loose microstructure of the untreated sample, the microstructure of the soil-RT sample is more compact and would have more ability to restrict the movement of water and air, creating a more robust and stable environment. In addition, the compacted blends with a higher concentration ratio of cement and RT compositionally show a higher content of aluminosilicates in the nanostructure of the gel and sodium cations, fulfilling the function of the network modifiers (balance of charges) product of the substitution of the silicon for the tetrahedral aluminates, as observed by Saldanha et al. [52].

The hydration and reaction processes of the cement for the formation of hydrates that bind soil particles and react with soil minerals, involve a complex series of chemical reactions, which can be affected by the presence of foreign matter or impurities, the relationship of water-cement, curing temperature, presence of additives, specific surface of the components (soil and cement), among others. The presence of water is an essential factor for the cement hydration process, at the same time, it guarantees the workability and manageability of the mixture that facilitates the processes of homogenization and compaction with the soil to be stabilized. As the RT residue is an industrialized material, sericite (a brittle mineral-see Figure 1) can affect the mechanical resistance of the soil-cement mixture.

In the soils of a cohesive nature (same as the present study) or with the presence of clay minerals (plastic fraction), the improvement in the strength can be carried out by the combined effect of the union and cementation of the particles through the cement hydration compounds (C-S-H) and by the processes of cation exchange, flocculation and pozzolanic reaction between the Ca^{2+} cations of the sodium hydroxide, formed during the hydration of the alite and belite, with the solubilized aluminates and silicates of the clay minerals [53]. Belite exists in six polymorphic structures, at the highest temperature of 1450 °C, it is found as α-belite; at 1425 °C it transforms into αH′-belite; at 1160 °C it becomes αL′-belite and at 650 °C it transforms into the β form, when cooled to room temperature, β-belite changes to γ-belite, its stable form. Due to the rate of cooling in manufacturing, the most common forms found in clinker are αL′-belite and β-belite [54,55]. When cement-soil react with water, alite and belite produce C-S-H (calcium silicate hydrate or tobermorite) and C-H (calcium hydroxide or portlandite), the C-H phase is well defined while the C/S ratio in C-S-H changes with the hydration time, which is at the maximum in the first second of contact with the water, releasing a high amount of heat that then decreases as the presence of silicates decreases. Thus, the cement's hydration and reaction processes for forming hydrates that bind soil particles and react with soil minerals, involve a complex series of chemical reactions still unknown and to be studied, which may be affected by the presence of foreign matter or impurities, the water-cement ratio, curing temperature, the presence of additives, and the specific surface of the components. Some of these reactions were possibly interrupted by the high addition of RT that caused the strength to decrease as a function of the porosity and the volumetric percentage of the cement.

5. Concluding Remarks

In this study, ground roof tile waste has been recycled as an additive in soil-cement mixtures. Moderate, medium, and high percentages of the RT residue have been added to the soil-cement submitted for 28-days of curing. According to the results obtained and the analyzes considering the influence of the porosity/cement ratio, the following conclusions can be drawn:

1. The objective of this article was to verify the impact of the porosity/cement ratio on the mechanical resistance of RT-soil-cement mixtures. When verifying the results, it is evident that the porosity/cement ratio adjusted to an exponent of 0.29 controls not only the unconfined compression but also the split tensile and the empirical relationship between these two;
2. The increase in the molding dry unit weight and the consequent reduction in the mixtures' porosity, significantly influenced the values obtained for the split tensile and compressive strength. This influence was visible in the inclination of the lines in the main effects graphs (see Figure 5);
3. A correlation of q_u and q_t with the index $\eta/C_{iv}^{0.29}$ resulted in excellent relations with coefficients of determination (R^2) between 93% and 98%. Even with the existence

of variability between the studied samples and the possibility of the occurrence of experimental errors, the approximations obtained are satisfactory;

4. By adding the RT recycled material, it was possible to demonstrate that the mixtures reached lower mechanical strengths as a function of $\eta/C_{iv}^{0.29}$, due to the presence of brittle minerals in the RT that delayed the hydration of the cement and the early development of the hydrated calcium aluminates. In addition, there is an intimate relationship between the cementing agent content and the molding moisture content, which results in a negative impact when considering certain dosages, in all mechanical tests;
5. The RT-cement-soil compacted blends with a higher concentration ratio of cement and RT compositionally, show a higher content of aluminosilicates in the gel nanostructure and sodium cations, fulfilling the function of the network modifier (balance of charges) product of the substitution of the silicon for the tetrahedral aluminates. The preceding can be correlated with the best mechanical responses of these mixtures in the presence of an adequate content of RT, to optimize the soil-cement system;
6. Since the samples prepared for the split tensile strength are the same as those for the simple compressive strength test, the coefficient of determination shows the exact significance of the main effects. Furthermore, it was possible to obtain a direct correlation between these tests, which was demonstrated as the ratio between the tensile strength and the simple compressive strength ($\xi = q_t/q_u$). The value obtained was 0.18. The ratio $\xi = q_t/q_u$ found a means that the tensile strength value by the diametral compression is equivalent to 18% of the simple compressive strength.

Author Contributions: Conceptualization, J.A.B. and C.M.-P.; methodology, J.A.B. and M.S.; validation, J.A.B., C.M.-P. and M.S.; formal analysis, J.A.B.; investigation, J.A.B.; resources, M.S.; writing—original draft preparation, J.A.B. and M.S.; writing—review and editing, M.S. and C.M.-P.; visualization, J.A.B.; supervision, J.A.B.; funding acquisition, J.A.B. All authors have read and agreed to the published version of the manuscript.

Funding: This study was financed in part by the Coordenação de Aperfeiçoamento de Pessoal de Nível Superior (CAPES)—Finance Code 001, CNPq and Fundação de Araucária do Paraná in Brazil.

Institutional Review Board Statement: Not applicable.

Informed Consent Statement: Not applicable.

Data Availability Statement: No further data is available.

Acknowledgments: The first Author want to thank the Federal University of Technology-Paraná for the support provided.

Conflicts of Interest: The authors declare no conflict of interest.

References

1. Baldovino, J.A.; Izzo, R.; Ekinci, A. Strength Relationship Equation for Artificially Stabilized Rammed Sedimentary Soils. *Buildings* **2022**, *12*, 1433. [CrossRef]
2. Onyelowe, K.C.; Ebid, A.M.; de Jesús Arrieta Baldovino, J.; Onyia, M.E. Hydraulic Conductivity Predictive Model of RHA-Ameliorated Laterite for Solving Landfill Liner Leachate, Soil and Water Contamination and Carbon Emission Problems. *Int. J. Low-Carbon Technol.* **2022**, *17*, 1134–1144. [CrossRef]
3. de Jesús Arrieta Baldovino, J.; dos Santos Izzo, R.L.; Ekinci, A. Strength, Durability, and Microstructure of Lime Production Residue Glass Powder Binder-Based Geomaterial. *Acta Geotech.* **2022**, 1–14. [CrossRef]
4. Horpibulsuk, S.; Chinkulkijniwat, A.; Cholphatsorn, A.; Suebsuk, J.; Liu, M.D. Consolidation Behavior of Soil–Cement Column Improved Ground. *Comput. Geotech.* **2012**, *43*, 37–50. [CrossRef]
5. Choobbasti, A.J.; Kutanaei, S.S. Microstructure Characteristics of Cement-Stabilized Sandy Soil Using Nanosilica. *J. Rock Mech. Geotech. Eng.* **2017**, *9*, 981–988. [CrossRef]
6. Lu, Y.; Liu, S.; Zhang, Y.; Li, Z.; Xu, L. Freeze-Thaw Performance of a Cement-Treated Expansive Soil. *Cold Reg. Sci. Technol.* **2020**, *170*, 102926. [CrossRef]
7. Narloch, P.; Woyciechowski, P. Assessing Cement Stabilized Rammed Earth Durability in A Humid Continental Climate. *Buildings* **2020**, *10*, 26. [CrossRef]

8. Lavat, A.E.; Trezza, M.A.; Poggi, M. Characterization of Ceramic Roof Tile Wastes as Pozzolanic Admixture. *Waste Manag.* **2009**, *29*, 1666–1674. [CrossRef]
9. Cabalar, A.F.; Hassan, D.I.; Abdulnafaa, M.D. Use of Waste Ceramic Tiles for Road Pavement Subgrade. *Road Mater. Pavement Des.* **2017**, *18*, 882–896. [CrossRef]
10. Robayo, R.A.; Mulford, A.; Munera, J.; Mejía de Gutiérrez, R. Alternative Cements Based on Alkali-Activated Red Clay Brick Waste. *Constr. Build. Mater.* **2016**, *128*, 163–169. [CrossRef]
11. Zhang, M.; Guo, H.; El-Korchi, T.; Zhang, G.; Tao, M. Experimental Feasibility Study of Geopolymer as the Next-Generation Soil Stabilizer. *Constr. Build. Mater.* **2013**, *47*, 1468–1478. [CrossRef]
12. Rios, S.; Cristelo, N.; Viana da Fonseca, A.; Ferreira, C. Stiffness Behavior of Soil Stabilized with Alkali-Activated Fly Ash from Small to Large Strains. *Int. J. Geomech.* **2017**, *17*, 04016087. [CrossRef]
13. Consoli, N.C.; Foppa, D.; Festugato, L.; Heineck, K.S. Key Parameters for Strength Control of Artificially Cemented Soils. *J. Geotech. Geoenvironmental Eng.* **2007**, *133*, 197–205. [CrossRef]
14. Lemos, S.G.F.P.; Almeida, M.d.S.S.; Consoli, N.C.; Nascimento, T.Z.; Polido, U.F. Field and Laboratory Investigation of Highly Organic Clay Stabilized with Portland Cement. *J. Mater. Civ. Eng.* **2020**, *32*, 04020063. [CrossRef]
15. Horpibulsuk, S.; Rachan, R.; Chinkulkijniwat, A.; Raksachon, Y.; Suddeepong, A. Analysis of Strength Development in Cement-Stabilized Silty Clay from Microstructural Considerations. *Constr. Build. Mater.* **2010**, *24*, 2011–2021. [CrossRef]
16. Li, X.; Rao, F.; Song, S.; Ma, Q. Effect of Cristobalite on the Mechanical Behaviour of Metakaolin-Based Geopolymer in Artificial Seawater. *Adv. Appl. Ceram.* **2020**, *119*, 29–36. [CrossRef]
17. Sun, Z.; Cui, H.; An, H.; Tao, D.; Xu, Y.; Zhai, J.; Li, Q. Synthesis and Thermal Behavior of Geopolymer-Type Material from Waste Ceramic. *Constr. Build. Mater.* **2013**, *49*, 281–287. [CrossRef]
18. Vogt, O.; Ukrainczyk, N.; Koenders, E. Effect of Silica Fume on Metakaolin Geopolymers' Sulfuric Acid Resistance. *Materials* **2021**, *14*, 5396. [CrossRef]
19. *ASTM D 2487-11*; Standard Practice for Classification of Soils for Engineering Purposes (Unified Soil Classification System). ASTM International: West Conshohocken, PA, USA, 2011; pp. 1–5. [CrossRef]
20. *ASTM D4318-10*; Stardard Test Methods for Liquid Limit, Plastic Limit and Plasticity Index of Soils. ASTM International: West Conshohocken, PA, USA, 2010.
21. *ASTM D 854-14*; Standard Test Methods for Specific Gravity of Soil Solids by Water Pycnometer 1. ASTM International: West Conshohocken, PA, USA, 2014.
22. *ABNT NBR 16605-17*; Cimento Portland e Outros Materiais Em Pó–Determinação Da Massa Específica. ABNT: São Paulo, Brazil, 2017.
23. Diambra, A.; Festugato, L.; Ibraim, E.; Peccin da Silva, A.; Consoli, N.C. Modelling Tensile/Compressive Strength Ratio of Artificially Cemented Clean Sand. *Soils Found.* **2018**, *58*, 199–211. [CrossRef]
24. Henzinger, C.; Schuhmacher, S.A.; Festugato, L. Applicability of the Porosity/Binder Index to Nonhomogeneous Mixtures of Fine-Grained Soil with Lignite Fly Ash. *J. Mater. Civ. Eng.* **2018**, *30*, 06018013. [CrossRef]
25. Mola-Abasi, H.; Shooshpasha, I. Influence of Zeolite and Cement Additions on Mechanical Behavior of Sandy Soil. *J. Rock Mech. Geotech. Eng.* **2016**, *8*, 746–752. [CrossRef]
26. Linhares, S.P.; Ferreira, J.A.; Ritter, E. Avaliação Da Implantação Da Resolução n. 307/2002 Do CONAMA Sobre Gerenciamento Dos Resíduos de Construção Civil. *Estud. Tecnológicos Em Eng.* **2007**, *3*, 176–194. [CrossRef]
27. Parliament, T.H.E.E.; Council, T.H.E.; The, O.F.; Union, E. Official Journal of the European Communities. *Anal. Proc.* **2000**, *21*, 196. [CrossRef]
28. Al-Bared, M.A.; Harahap, I.S.; Marto, A.; Abad SV AN, K.; Mustaffa, Z.; Ali, M.O. Mechanical behaviour of waste powdered tiles and Portland cement treated soft clay. *Geomech. Eng.* **2019**, *19*, 37–47. [CrossRef]
29. *ABNT NBR 7182*; Solo-Ensaio de Compactação. Assossiação Brasileira de Normas Técnicas: São Paulo, Brazil, 2016.
30. Consoli, N.C.; Quiñonez, R.A.; González, L.E.; López, R.A.; Quiñónez, R.A.; González, L.E.; López, R.A.; Quiñonez, R.A.; González, L.E.; López, R.A.; et al. Influence of Molding Moisture Content and Porosity/Cement Index on Stiffness, Strength, and Failure Envelopes of Artificially Cemented Fine-Grained Soils. *J. Mater. Civ. Eng.* **2016**, *29*, 1–10. [CrossRef]
31. Baldovino, J.D.J.A.; Moreira, E.B.; Carazzai, É.; Rocha, E.V.D.G.; dos Santos Izzo, R.; Mazer, W.; Rose, J.L. Equations Controlling the Strength of Sedimentary Silty Soil–Cement Blends: Influence of Voids/Cement Ratio and Types of Cement. *Int. J. Geotech. Eng.* **2021**, *15*, 359–372. [CrossRef]
32. Consoli, N.C.; Marques, S.F.V.; Floss, M.F.; Festugato, L. Broad-Spectrum Empirical Correlation Determining Tensile and Compressive Strength of Cement-Bonded Clean Granular Soils. *J. Mater. Civ. Eng.* **2017**, *29*, 1–7. [CrossRef]
33. Consoli, N.C.; Dalla Rosa, A.; Corte, M.B.; Lopes, L.D.S., Jr.; Consoli, B.S. Porosity-Cement Ratio Controlling Strength of Artificially Cemented Clays. *J. Mater. Civ. Eng.* **2011**, *23*, 1249–1254. [CrossRef]
34. Consoli, N.C.; Rosa, D.A.; Cruz, R.C.; Rosa, A.D. Water Content, Porosity and Cement Content as Parameters Controlling Strength of Artificially Cemented Silty Soil. *Eng. Geol.* **2011**, *122*, 328–333. [CrossRef]
35. Herbudiman, B.; Saptaji, A.M. Self-Compacting Concrete with Recycled Traditional Roof Tile Powder. *Procedia Eng.* **2013**, *54*, 805–816. [CrossRef]
36. Miličević, I.; Štirmer, N.; Bjegović, D. Optimisation of Concrete Mixtures Made with Crushed Clay Bricks and Roof Tiles. *Mag. Concr. Res.* **2015**, *67*, 109–120. [CrossRef]

37. Dondi, M.; Guarini, G.; Raimondo, M.; Zanelli, C. Recycling PC and TV Waste Glass in Clay Bricks and Roof Tiles. *Waste Manag.* **2009**, *29*, 1945–1951. [CrossRef]
38. *ASTM D 2166-03*; Standard Test Method for Unconfined Compressive Strength of Cohesive Soil 1. ASTM International: West Conshohocken, PA, USA, 2003; Volume 4.
39. *ABNT NBR 7222*; Concreto e Argamassa—Determinação Da Resistência à Tração Por Compressão Diametral de Corpos de Prova Cilíndricos. ABNT: São Paulo, Brazil, 2011.
40. Larnach, W.J. Relationship between Dry Density, Voids/Cement Ratio and the Strength of Soil-Cement Mixtures. *Civil Eng. Public Works Rev./UK* **1960**, *60*, 903–905.
41. Diambra, A.; Ibraim, E.; Peccin, A.; Consoli, N.C.; Festugato, L. Theoretical Derivation of Artificially Cemented Granular Soil Strength. *J. Geotech. Geoenvironmental. Eng.* **2017**, *143*, 04017003. [CrossRef]
42. Meurant, G. *Soil Mechanics of Earthworks, Foundations and Highway Engineering*; Elsevier: Amsterdam, The Netherlands, 2013; ISBN 9781483291819.
43. Consoli, N.C.; Cruz, R.C.; Floss, M.F.; Festugato, L. Parameters Controlling Tensile and Compressive Strength of Artificially Cemented Sand. *J. Geotech. Geoenvironmental. Eng.* **2010**, *136*, 759–763. [CrossRef]
44. Consoli, N.C. A Method Proposed for the Assessment of Failure Envelopes of Cemented Sandy Soils. *Eng. Geol.* **2014**, *169*, 61–68. [CrossRef]
45. Consoli, N.C.; Scheuermann, H.C.; Godoy, V.B.; Rosenbach, C.M.D.C.; Carraro, J.J.A.H. Durability of RAP-Industrial Waste Mixtures Under Severe Climate Conditions. *Soils Rocks* **2018**, *41*, 149–156. [CrossRef]
46. Filho, H.C.S.; Martins, C.G.; Menezes, R.J.W.; Dornelles, L.E.; Consoli, N.C. The Effect of Key Parameters on the Strength of a Dispersive Soil Stabilized with Sustainable Binders. *Geotech. Geol. Eng.* **2021**, *39*, 5395–5404. [CrossRef]
47. Pereira dos Santos, C.; Bruschi, G.J.; Mattos, J.R.G.; Consoli, N.C. Stabilization of Gold Mining Tailings with Alkali-Activated Carbide Lime and Sugarcane Bagasse Ash. *Transp. Geotech.* **2022**, *32*, 100704. [CrossRef]
48. Al-Subari, L.; Ekinci, A. Strength and durability assessment of shredded tire rubber stabilized artificially cemented alluvial clay. *Constr. Build. Mater.* **2022**, *345*, 128312. [CrossRef]
49. Consoli, N.C.; Vaz Ferreira, P.M.; Tang, C.S.; Veloso Marques, S.F.; Festugato, L.; Corte, M.B. A Unique Relationship Determining Strength of Silty/Clayey Soils-Portland Cement Mixes. *Soils Found.* **2016**, *56*, 1082–1088. [CrossRef]
50. Baldovino, J.A.; Moreira, E.B.; Izzo, R.L.D.S.; Rose, J.L. Empirical Relationships with Unconfined Compressive Strength and Split Tensile Strength for the Long Term of a Lime-Treated Silty Soil. *J. Mater. Civ. Eng.* **2018**, *30*, 06018008. [CrossRef]
51. Bonaccorsi, E.; Merlino, S. Modular Microporous Minerals: Cancrinite-Davyne Group and C-S-H Phases. In *Micro- and Mesoporous Mineral Phases*; De Gruyter: Berlin, Germany; Boston, MA, USA, 2018; Volume 57, pp. 241–290. [CrossRef]
52. Saldanha, R.B.; da Rocha, C.G.; Caicedo, A.M.L.; Consoli, N.C. Technical and Environmental Performance of Eggshell Lime for Soil Stabilization. *Constr. Build. Mater.* **2021**, *298*, 123648. [CrossRef]
53. Lade, P.V.; Trads, N. The Role of Cementation in the Behaviour of Cemented Soils. *Geotech. Res.* **2014**, *1*, 111–132. [CrossRef]
54. Izadifar, M.; Ukrainczyk, N.; Salah Uddin, K.M.; Middendorf, B.; Koenders, E. Dissolution of β-C2S Cement Clinker: Part 2 Atomistic Kinetic Monte Carlo (KMC) Upscaling Approach. *Materials* **2022**, *15*, 6716. [CrossRef]
55. Kacimi, L.; Simon-Masseron, A.; Salem, S.; Ghomari, A.; Derriche, Z. Synthesis of Belite Cement Clinker of High Hydraulic Reactivity. *Cem. Concr. Res.* **2009**, *39*, 559–565. [CrossRef]